

Supporting Information for:

Oxygen transport and isotopic exchange in iron oxide/YSZ thermochemically-active materials *via* splitting of C(¹⁸O)₂ at high temperature studied by thermogravimetric analysis and secondary ion mass spectrometry

Eric N. Coker, James A. Ohlhausen, Andrea Ambrosini and James E. Miller

A) Thermogravimetric analysis of ¹⁸O-labelled 8YSZ

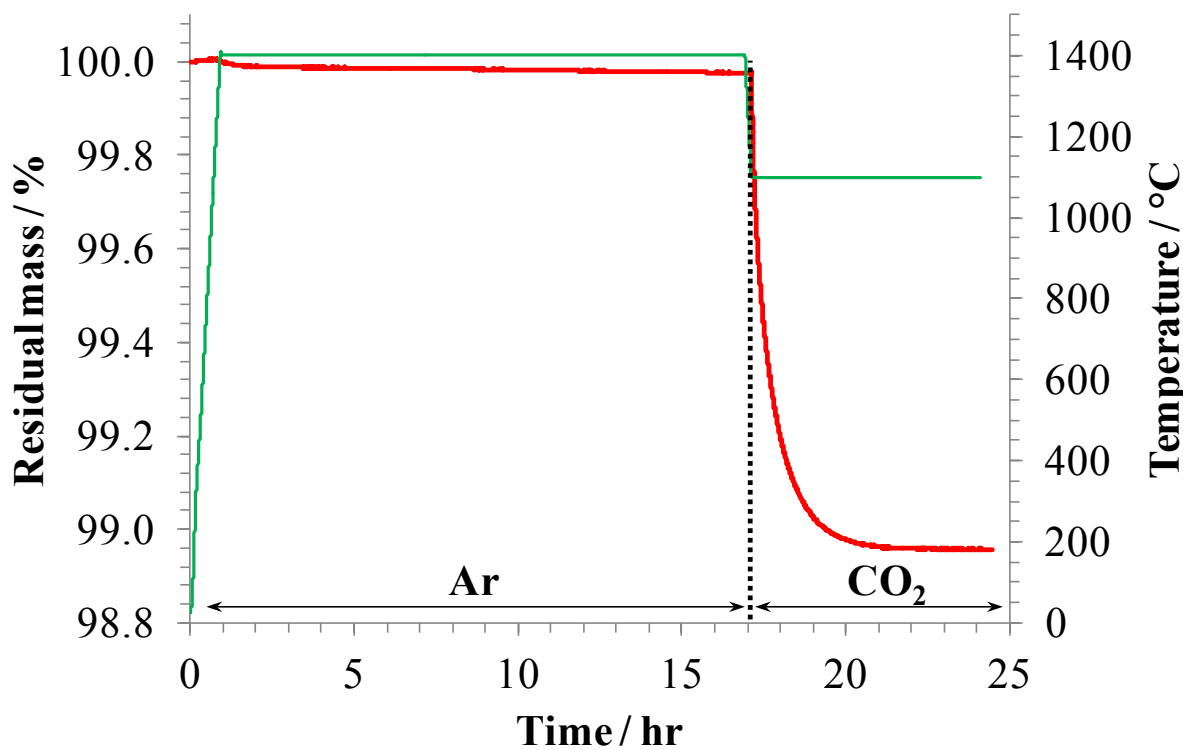


Figure S1. Thermogravimetric data for an ¹⁸O-enriched 8YSZ sample without added iron during thermochemical cycling. To enrich sample with ¹⁸O, it was held at 1400 °C for 16 hr under Ar, then exposed to C(¹⁸O)₂ at 1100 °C for 1 hr.

B) Time-of-Flight Secondary Ion Mass Spectrometry; multivariate analysis

Experimental details

Sample preparation and image acquisition

After ^{18}O labeling each sample was cross-sectioned, then polished with clean metallographic procedures to prevent cross contamination from other polishing processes. The samples were mounted and polished in epoxy. Following polishing, the bulk epoxy was removed to reduce vacuum out-gassing in preparation for surface analysis. Samples were analyzed by Time-of-Flight Secondary Ion Mass Spectrometry (ToF-SIMS) using a TOF.SIMS 5 instrument manufactured by IonTOF GmbH of Münster, Germany. Two random areas were analyzed from near the center of each sample. Prior to analysis, each analysis area was pre-sputtered with 2kV Cs^+ ions until a bulk structure was encountered as measured by a removal of surface hydrocarbon species. After surface cleaning, each area was analyzed with 25kV Bi_3^{++} source in BA-Image mode. Negative secondary ions from a $100 \times 100 \mu\text{m}^2$ area were analyzed by integrating 500 frames over a 256x256 pixel array. The resulting spectrum image data (full spectrum at every pixel) were processed using Sandia's multivariate analysis toolkit (AXSIA).^{1,2} In multivariate analysis, the spectrum image is decomposed into components each consisting of spectral and concentration (image) constituents. For each image, the component relating to the location of the FeO_x particles was used to determine an image mask, which was subsequently applied to images during processing. ^{16}O and ^{18}O plots and ratios are used to determine the extent of intentional oxidation of the embedded FeO_x particles. For reference, the natural abundance ratio of $^{16}\text{O}/^{18}\text{O}$ is about 500.

Multivariate analysis

Figure S2 shows a series of images from ToF-SIMS representing various stages of the multivariate analysis used to isolate oxygen isotope distribution data for the iron oxide particles within the YSZ matrix. The images are all of one area in sample CP-12 (11.7 mol-% Fe/8YSZ, prepared by co-precipitation). Images A and B show the total ^{16}O and ^{18}O intensities, respectively, regardless of their chemical origin. Image C is a composite image of the

multivariate results from the specimen. In this figure, each chemical component is displayed with unique colours; purple is due to the YSZ matrix, green shows voids in the sample, blue is due to iron oxide particles, and cyan is internal contamination. Each component has an associated spectrum, but only the spectrum for the iron oxide particles is selected in the development of a sample mask. In this spectrum, we see both isotopes of oxygen as oxygen atom fragments and as FeO_x fragments. Note that the variations in relative ^{16}O to ^{18}O concentrations are not separated in the multivariate analysis. This will be done later with the raw data. The blue component is used to identify the location of Fe oxide particles by creating a mask that is applied to raw oxygen intensities, as shown in image D. Application of the mask to the raw data from images A and B produces images E (^{16}O) and F (^{18}O), where only signals emanating from iron oxide particles are seen above background. Finally, the ratios of intensities of ^{16}O and ^{18}O are calculated, and are displayed in images G ($^{16}\text{O}/^{18}\text{O}$) and H ($^{18}\text{O}/^{16}\text{O}$) to highlight contrast in the distribution of the two isotopes.

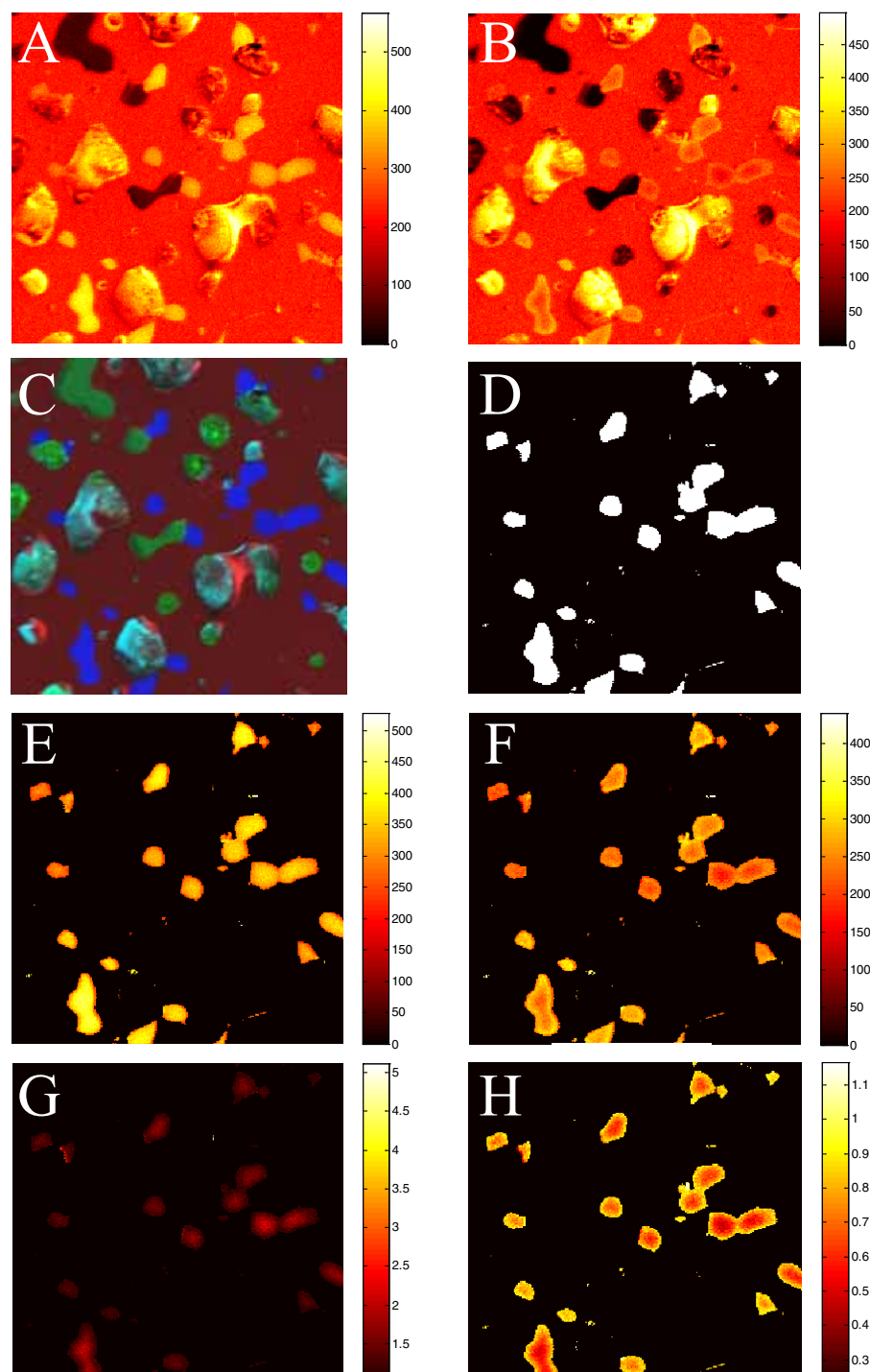


Figure S2. Images of sample CP-12 illustrating the various steps in the multivariate analysis procedure. A: ^{16}O signal (non chemical-specific); B: ^{18}O signal (non chemical-specific); C: $^{16}\text{O} + ^{18}\text{O}$ map (blue = FeO_x ; purple = YSZ; green = voids; cyan = debris); D: Mask selecting only FeO_x ; E: ^{16}O masked signal; F: ^{18}O masked signal; G: $^{16}\text{O}/^{18}\text{O}$ ratio, masked; H: $^{18}\text{O}/^{16}\text{O}$ ratio, masked.

C) ToF-SIMS images of ^{16}O distribution and $^{16}\text{O}/^{18}\text{O}$ ratios

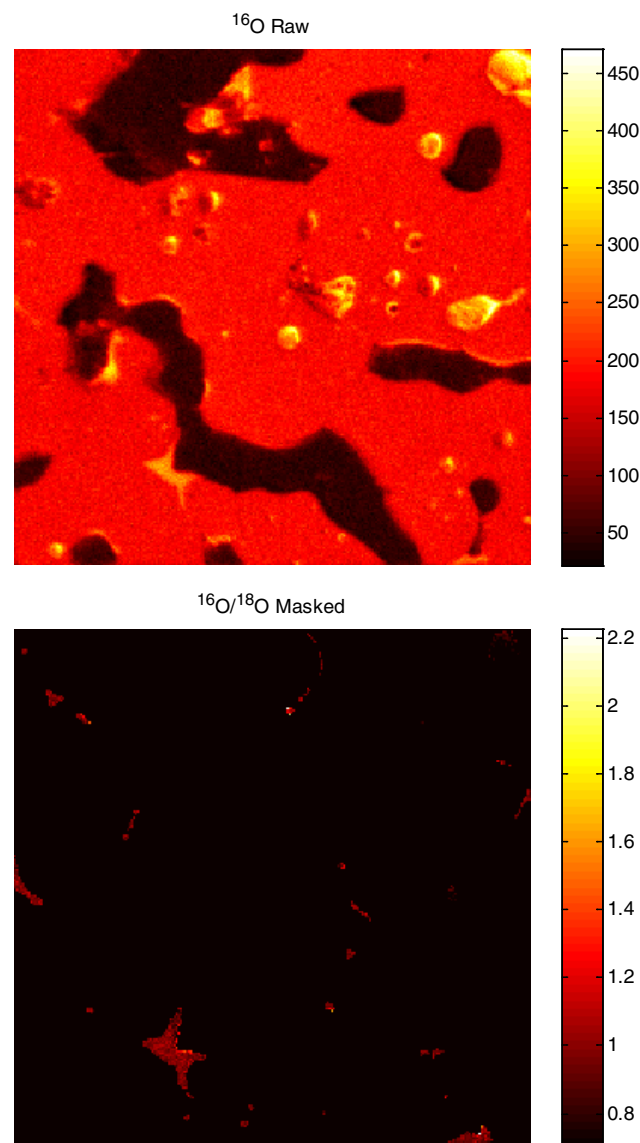


Figure S3. ToF-SIMS images of ^{16}O distribution (top) and masked $^{16}\text{O}/^{18}\text{O}$ ratio (bottom) for sample CP-7.

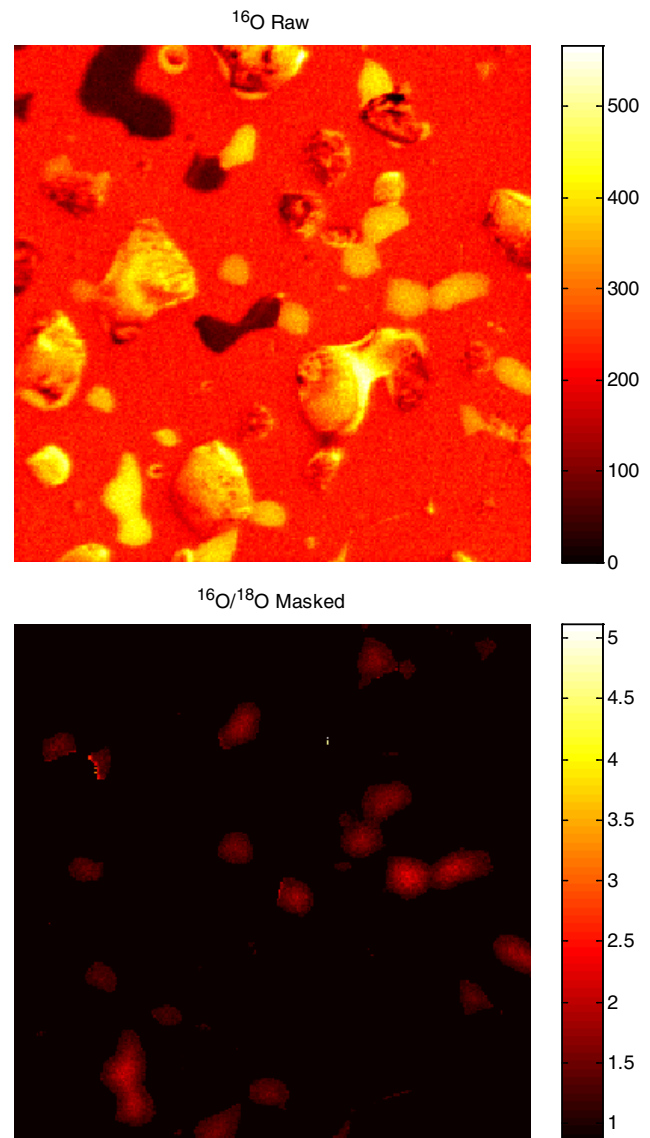


Figure S4. ToF-SIMS images of ^{16}O distribution (top) and masked $^{16}\text{O}/^{18}\text{O}$ ratio (bottom) for sample CP-12.

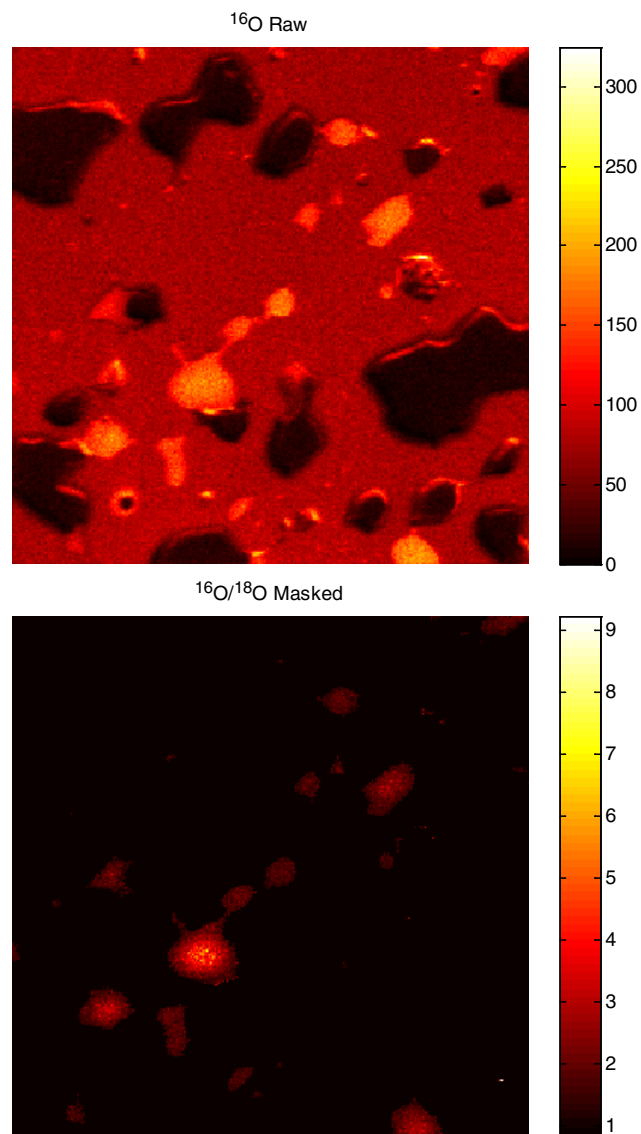


Figure S5. ToF-SIMS images of ^{16}O distribution (top) and masked $^{16}\text{O}/^{18}\text{O}$ ratio (bottom) for sample CP-15.

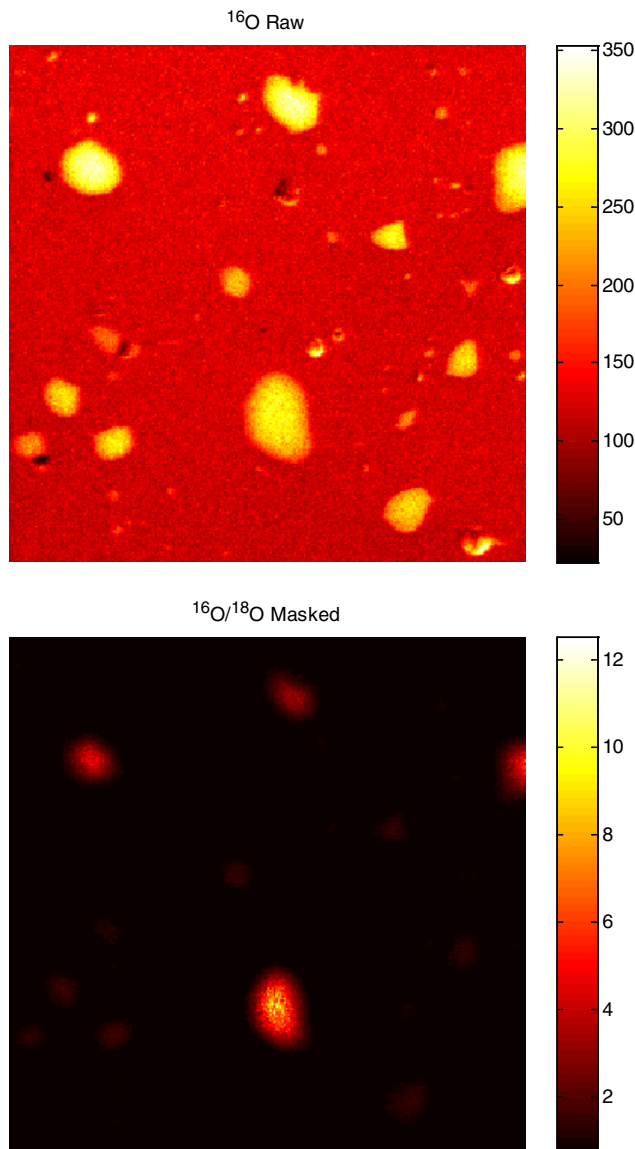


Figure S6. ToF-SIMS images of ^{16}O distribution (top) and masked $^{16}\text{O}/^{18}\text{O}$ ratio (bottom) for sample SS-15.

D) ToF-SIMS multivariate analysis of YSZ dissolution into iron oxide

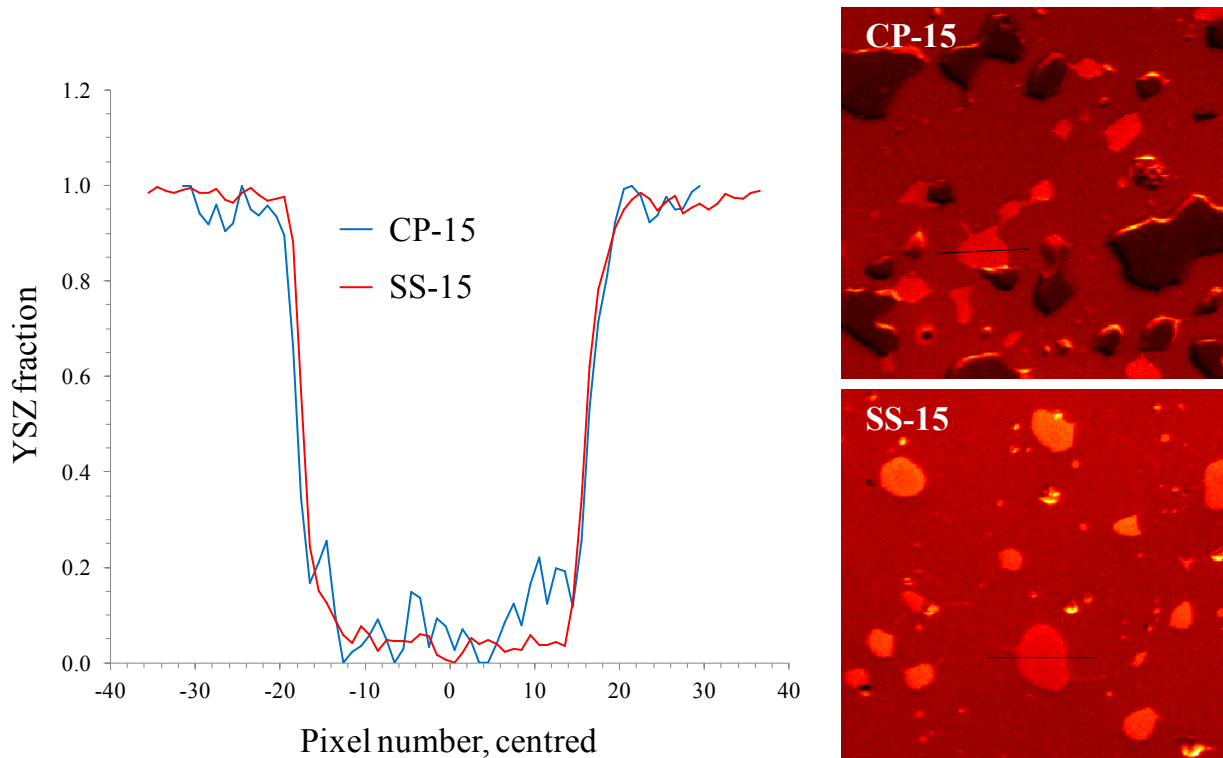


Figure S7. Line scans of fractional YSZ component derived through multivariate analysis of ToF-SIMS images. The scan lines are indicated in the respective colour images. Distance is measured in pixels, with the zero position close to the centre of the particle.

The YSZ fraction is calculated by defining the intensity of the YSZ component determined by multivariate analysis and the intensity of the iron oxide component as determined by multivariate analysis on a pixel-by-pixel basis. Therefore, linescans were made at the same locations in both the iron oxide and YSZ component images. The percent YSZ from the total of (YSZ + iron oxide) was calculated. This is not a quantitative determination, but merely an attempt to determine the relative amount of YSZ in iron oxide particles and *vice versa* from sample to sample.

E) Density measurement of sample disc fragments through pycnometry

Experimental details

Helium pycnometry was performed using a Micromeritics AccuPyc 1330. A piece of sintered pellet (approximately 400 mg) was weighed out and loaded into a 1 cm³ sample holder, which was capped and placed into the pycnometer. The volume of the sample was measured three times *via* gas displacement in the sample holder. The gas displacement density was calculated by dividing the volume of the sample by its mass. The AccuPyc works by measuring the amount of displaced gas. The pressures observed upon filling the sample chamber and then discharging it into a second empty chamber allow computation of the sample solid phase volume. Helium molecules fill the pores of the sample; only the truly solid phase and any closed pores of the sample (*i.e.*, those not accessible to the gas phase) displace the He. The instrument was calibrated before measurements, and at regular intervals during measurements. Calibration was achieved by placing a standard solid object with certified volume into the sample chamber and running a measurement.

Results

Since helium is able to permeate small pores in the samples, the presence of such interconnected pores does not result in a reduction in measured density. Only closed voids without access to the gas phase contribute to lowering the measured density by this method. The estimated approach to theoretical density values listed in Table S1 should be considered upper limits to the possible values, since a constant density of 8YSZ of 6.1 g cm⁻³ was used for the calculations, regardless of the amount of iron dissolved in the 8YSZ. Dissolution of iron into 8YSZ has been shown to decrease the unit cell volume of 8YSZ, therefore increasing its bulk density.³

Table S1. Summary of average densities of sample fragments measured by helium pycnometry

Sample	Gas-displacement density / g cm ⁻³	Approach to theoretical density ^a / %
CP-7	5.79	95.0
CP-12	5.69	93.3
CP-15	5.74	94.1
SS-15	5.78	94.8

^a Assuming fully dense 8YSZ has a density of 6.1 g cm⁻³, and discounting any change in density of 8YSZ due to iron dissolution.

References

- 1 J.A. Ohlhausen, M.R. Keenan, P.G. Kotula and D.E. Peebles, *Appl. Surf. Sci.* 2004, **231-232**, 230-234.
- 2 M.R. Keenan, V.S. Smentkowski, J.A. Ohlhausen and P.G. Kotula, *Surf. Interface Anal.* 2008, **40**, 97–106.
- 3 E.N. Coker, A. Ambrosini, M.A. Rodriguez and J.E. Miller, *J. Mater. Chem.*, 2011, **21**, 10767-76.